

## A Lepton Universality Test at CERN NA62 Experiment

Evgueni Goudzovski

*School of Physics and Astronomy, University of Birmingham,  
Edgbaston, Birmingham, B15 2TT, United Kingdom*

The NA62 experiment at CERN collected a large sample of  $K^+ \rightarrow e^+ \nu$  decays during a dedicated run in 2007, aiming at a precise test of lepton universality by measurement of the helicity suppressed ratio  $R_K = \Gamma(K^+ \rightarrow e^+ \nu) / \Gamma(K^+ \rightarrow \mu^+ \nu)$ . The preliminary result of the analysis of a partial data sample of 51089  $K^+ \rightarrow e^+ \nu$  candidates is  $R_K = (2.500 \pm 0.016) \times 10^{-5}$ , which is consistent with the Standard Model expectation.

### Introduction

Due to the  $V - A$  structure of the weak interactions, the Standard Model (SM) rates of the leptonic meson decays  $P^+ \rightarrow \ell^+ \nu$  are helicity suppressed. Within the two-Higgs doublet models (2HDM), which is a wide class of models including the minimum supersymmetric (SUSY) one, the charged Higgs boson ( $H^\pm$ ) exchange induces a tree-level contribution to (semi)leptonic decays proportional to the Yukawa couplings of quarks and leptons<sup>1</sup>. In  $P^+ \rightarrow \ell^+ \nu$  decays, the  $H^\pm$  exchange can compete with the  $W^\pm$  exchange, thanks to the above suppression.

At tree level, the  $H^\pm$  exchange contribution to  $P^+ \rightarrow \ell^+ \nu$  decay widths (with  $P = \pi, K, B$ ) is lepton flavour independent, and is approximately described by<sup>2</sup>

$$\frac{\Delta \Gamma(P^+ \rightarrow \ell^+ \nu)}{\Gamma^{\text{SM}}(P^+ \rightarrow \ell^+ \nu)} \approx -2 \left( \frac{M_P}{M_H} \right)^2 \frac{\tan^2 \beta}{1 + \varepsilon_0 \tan \beta}. \quad (1)$$

Here  $M_H$  is the charged Higgs boson mass,  $\tan \beta$  is the ratio of vacuum expectation values of the two Higgs doublets, a fundamental parameter controlling the charged Higgs couplings, and  $\varepsilon_0 \sim 10^{-2}$  is an effective coupling. For a reasonable choice of the parameters ( $\tan \beta = 40$ ,  $M_H = 500 \text{ GeV}/c^2$ ), one expects  $\sim 30\%$  relative suppression of  $B^+ \rightarrow \ell^+ \nu$  decays, and  $\sim 0.3\%$  suppression of  $K^+ \rightarrow \ell^+ \nu$  decays. However the searches for new physics in these decay rates are hindered by the uncertainties of their SM predictions.

On the other hand, the ratio of kaon leptonic decay rates  $R_K = \Gamma(K_{e2}) / \Gamma(K_{\mu 2})$ , where the notation  $K_{\ell 2}$  is adopted for the  $K^+ \rightarrow \ell^+ \nu$  decays, has been calculated with an excellent accuracy within the SM<sup>3</sup>:

$$R_K^{\text{SM}} = (m_e / m_\mu)^2 \left( \frac{m_K^2 - m_e^2}{m_K^2 - m_\mu^2} \right)^2 (1 + \delta R_{\text{QED}}) = (2.477 \pm 0.001) \times 10^{-5}. \quad (2)$$

Here  $\delta R_{\text{QED}} = (-3.78 \pm 0.04)\%$  is a correction due to the inner bremsstrahlung (IB)  $K_{\ell 2 \gamma}$  process. The ratio  $R_K$  is sensitive to lepton flavour universality violation (LFV) effects originating at one-loop level from  $H^\pm$  exchange in 2HDM<sup>4,5</sup>, and the mixing effects in the right-handed

slepton sector, providing a unique probe into this aspect of supersymmetric flavour physics<sup>6</sup>.  $R_K$  receives the following leading-order contribution due to LFV coupling of the Higgs boson:

$$\frac{\Delta R_K}{R_K^{\text{SM}}} = \left(\frac{M_K}{M_H}\right)^4 \left(\frac{M_\tau}{M_e}\right)^2 |\Delta_R^{31}|^2 \tan^6 \beta, \quad (3)$$

where  $|\Delta_R^{31}|$  is the mixing parameter between the superpartners of the right-handed leptons, which can reach  $\sim 10^{-3}$ . This can enhance  $R_K$  by  $\mathcal{O}(1\%)$  relative, with no contradiction to presently known experimental constraints (including upper bounds on the LFV  $\tau \rightarrow eX$  decays with  $X = \eta, \gamma, \mu\mu$ ).

The current world average (including only final results, and thus ignoring the preliminary NA48/2 ones) is  $R_K^{\text{WA}} = (2.490 \pm 0.030) \times 10^{-5}$ , dominated by a recent measurement by the KLOE collaboration<sup>8</sup>. The NA62 experiment at CERN collected a dedicated data sample in 2007–08, aiming at a measurement of  $R_K$  with a 0.4% precision. The preliminary result obtained with a partial data sample is presented here.

## 1 Beam, detector and data taking

The beam line and setup of the NA48/2 experiment<sup>9</sup> were used for the NA62 2007–08 data taking. Experimental conditions and trigger logic were optimized for the  $K_{e2}/K_{\mu2}$  measurement.

The beam line is capable of delivering simultaneous unseparated  $K^+$  and  $K^-$  beams derived from 400 GeV/c primary protons extracted from the CERN SPS. Most of the data, including the sample used for the present analysis, were collected with the  $K^+$  beam only, as the muon sweeping system provides better suppression of the positive beam halo component. A narrow momentum band of  $(74.0 \pm 1.6)$  GeV/c was used to minimize the corresponding contribution to resolution in kinematical variables.

The fiducial decay region is contained in a 114 m long cylindrical vacuum tank. With  $1.8 \times 10^{12}$  primary protons incident on the target per SPS pulse of 4.8 s duration, the beam flux at the entrance to the decay volume is  $2.5 \times 10^7$  particles per pulse. The fractions of  $K^+$ ,  $\pi^+$ ,  $p$ ,  $e^+$  and  $\mu^+$  in the beam are 0.05, 0.63, 0.21, 0.10 and 0.01, respectively. The fraction of beam kaons decaying in the vacuum tank at nominal momentum is 18%. The transverse size of the beam within the decay volume is  $\delta x = \delta y = 7$  mm (rms), and its angular divergence is negligible.

Among the subdetectors located downstream the decay volume, a magnetic spectrometer, a plastic scintillator hodoscope (HOD) and a liquid krypton electromagnetic calorimeter (LKr) are principal for the measurement. The spectrometer, used to detect charged products of kaon decays, is composed of four drift chambers (DCHs) and a dipole magnet. The HOD producing fast trigger signals consists of two planes of strip-shaped counters. The LKr, used for particle identification and as a veto, is an almost homogeneous ionization chamber,  $27X_0$  deep, segmented transversally into 13,248 cells ( $2 \times 2$  cm<sup>2</sup> each), and with no longitudinal segmentation. A beam pipe traversing the centres of the detectors allows undecayed beam particles and muons from decays of beam pions to continue their path in vacuum.

A minimum bias trigger configuration is employed, resulting in high efficiency with relatively low purity. The  $K_{e2}$  trigger condition consists of coincidence of hits in the HOD planes (the so called  $Q_1$  signal) with 10 GeV LKr energy deposition. The  $K_{\mu2}$  trigger condition consists of the  $Q_1$  signal alone downscaled by a factor of 150. Loose lower and upper limits on DCH activity are also applied.

The main data taking took place during four months starting in June 2007. Two additional weeks of data taking allocated in September 2008 were used to collect special data samples for studies of systematic effects. The present analysis is based on  $\sim 40\%$  of the data sample.

## 2 Analysis strategy and event selection

The analysis strategy is based on counting the numbers of reconstructed  $K_{e2}$  and  $K_{\mu2}$  candidates collected concurrently. Consequently the result does not rely on kaon flux measurement, and several systematic effects (e.g. due to reconstruction and trigger efficiencies, time-dependent effects) cancel to first order.

To take into account the significant dependence of signal acceptance and background level on lepton momentum, the measurement is performed independently in bins of this observable: 10 bins covering a lepton momentum range of  $[15; 65]$  GeV/ $c$  are used. The ratio  $R_K$  in each bin is computed as

$$R_K = \frac{1}{D} \cdot \frac{N(K_{e2}) - N_B(K_{e2})}{N(K_{\mu2}) - N_B(K_{\mu2})} \cdot \frac{A(K_{\mu2})}{A(K_{e2})} \cdot \frac{f_\mu \times \epsilon(K_{\mu2})}{f_e \times \epsilon(K_{e2})} \cdot \frac{1}{f_{\text{LKr}}}, \quad (4)$$

where  $N(K_{\ell2})$  are the numbers of selected  $K_{\ell2}$  candidates ( $\ell = e, \mu$ ),  $N_B(K_{\ell2})$  are numbers of background events,  $A(K_{\mu2})/A(K_{e2})$  is the geometric acceptance correction,  $f_\ell$  are efficiencies of  $e/\mu$  identification,  $\epsilon(K_{\ell2})$  are trigger efficiencies,  $f_{\text{LKr}}$  is the global efficiency of the LKr readout, and  $D = 150$  is the downscaling factor of the  $K_{\mu2}$  trigger.

A detailed Monte Carlo (MC) simulation including beam line optics, full detector geometry and material description, stray magnetic fields, local inefficiencies of DCH wires, and time variations of the above throughout the running period, is used to evaluate the acceptance correction  $A(K_{\mu2})/A(K_{e2})$  and the geometric parts of the acceptances for background processes entering the computation of  $N_B(K_{\ell2})$ . The  $K_{\ell2(\gamma)}$  processes are simulated in one-photon approximation<sup>3</sup>; the resummation of leading logarithms<sup>10</sup> is neglected at this stage. Simulations are used to a limited extent only: particle identification, trigger and readout efficiencies are measured directly.

Due to topological similarity of  $K_{e2}$  and  $K_{\mu2}$  decays, a large part of the selection conditions is common for both decays: (1) exactly one reconstructed particle of positive electric charge; (2) its momentum  $15 \text{ GeV}/c < p < 65 \text{ GeV}/c$  (the lower limit is due to the 10 GeV LKr energy deposit trigger requirement in  $K_{e2}$  trigger); (3) extrapolated track impact points in DCH, LKr and HOD are within their geometrical acceptances; (4) no LKr energy deposition clusters with energy  $E > 2 \text{ GeV}$  and not associated to the track to suppress background from other kaon decays; (5) distance between the charged track and the nominal kaon beam axis  $\text{CDA} < 3 \text{ cm}$ , decay vertex longitudinal position within the nominal decay volume (the latter condition is optimized in each lepton momentum bin).

The following two principal selection criteria are different for the  $K_{e2}$  and  $K_{\mu2}$  decays.  $K_{\ell2}$  kinematic identification is based on the reconstructed squared missing mass assuming the track to be a positron or a muon:  $M_{\text{miss}}^2(\ell) = (P_K - P_\ell)^2$ , where  $P_K$  and  $P_\ell$  ( $\ell = e, \mu$ ) are the four-momenta of the kaon (average beam momentum assumed) and the lepton (positron or muon mass assumed). A selection condition  $|M_{\text{miss}}^2(e)| < M_0^2$  is applied to select  $K_{e2}$  candidates, and  $|M_{\text{miss}}^2(\mu)| < M_0^2$  for  $K_{\mu2}$  ones, where  $M_0^2$  varies from 0.009 to 0.013 (GeV/ $c^2$ )<sup>2</sup> among lepton momentum bins depending on  $M_{\text{miss}}^2$  resolution. Particle identification is based on the ratio  $E/p$  of track energy deposit in the LKr calorimeter to its momentum measured by the spectrometer. Particles with  $0.95 < E/p < 1.1$  ( $E/p < 0.85$ ) are identified as positrons (muons).

## 3 Backgrounds

**$K_{\mu2}$  decay** with a mis-identified muon is the main background source in the  $K_{e2}$  sample. Sufficient kinematic separation of  $K_{e2}$  and  $K_{\mu2}$  decays is not achievable at high lepton momentum ( $p > 30 \text{ GeV}/c$ ), as shown in Fig. 1a. The probability of muon identification as positron in that momentum range ( $E/p > 0.95$  due to ‘catastrophic’ bremsstrahlung in or in front of the LKr) is  $P(\mu \rightarrow e) \sim 4 \times 10^{-6}$ , which is non-negligible compared to  $R_K^{\text{SM}} = 2.477 \times 10^{-5}$ . A direct

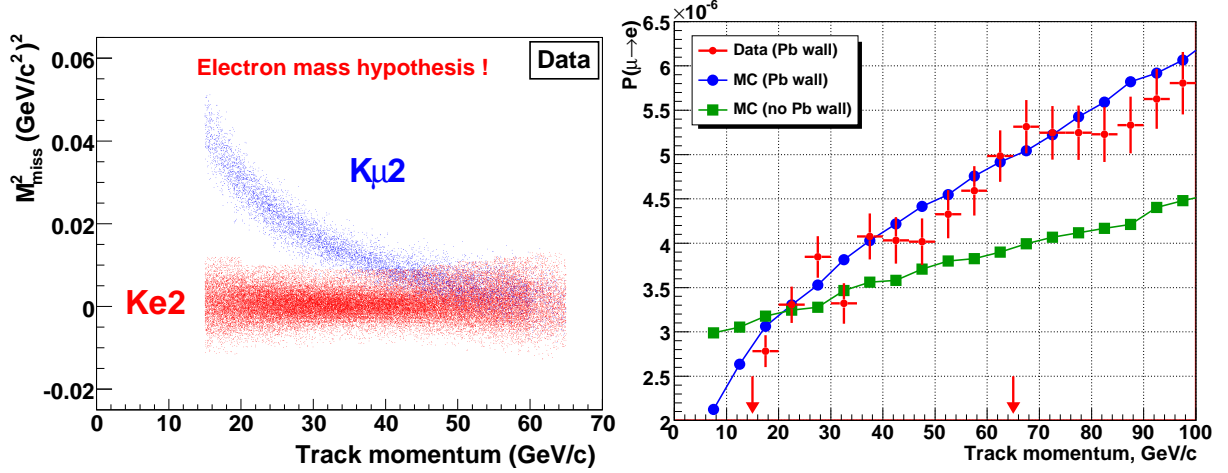


Figure 1: (a) Missing mass squared in positron hypothesis  $M_{\text{miss}}^2(e)$  vs lepton momentum for reconstructed  $K_{e2}$  and  $K_{\mu2}$  decays: kinematic separation of  $K_{e2}$  and  $K_{\mu2}$  decays is possible at low lepton momentum only. (b) Measured and simulated probability of muon identification as electron/positron  $P(\mu \rightarrow e)$  vs its momentum: data with the Pb wall, MC simulations with and without the Pb wall (the signal region is marked with arrows).

measurement of  $P(\mu \rightarrow e)$  to  $\sim 10^{-2}$  relative precision is necessary to validate the theoretical calculation of the bremsstrahlung cross-section<sup>11</sup> in the high  $\gamma$  energy range used to evaluate the  $K_{\mu2}$  background.

The available muon samples are typically affected by  $\sim 10^{-4}$  electron/positron contamination due to  $\mu \rightarrow e$  decays in flight, which obstructs the  $P(\mu \rightarrow e)$  measurements. In order to obtain sufficiently pure muon samples, a  $9.2X_0$  thick lead (Pb) wall covering  $\sim 20\%$  of the geometric acceptance was installed in front of the LKr calorimeter (between the two HOD planes) during a period of the data taking. In the samples of tracks traversing the Pb and having  $E/p > 0.95$ , the electron component is suppressed to a level of  $\sim 10^{-7}$  by energy losses in Pb.

The momentum dependence of  $P(\mu \rightarrow e)$  for muons traversing the Pb has been measured with a data sample collected during a special muon ( $\mu^\pm$ ) run of 20h duration, and compared to the results of a dedicated Geant4-based MC simulation of the region downstream the spectrometer involving standard energy loss processes and bremsstrahlung<sup>11</sup>. The data/MC comparison (Fig. 1b) shows good agreement in a wide momentum range within statistical errors, which validates the cross-section calculation at the corresponding precision level. The simulation shows that the Pb wall modifies  $P(\mu \rightarrow e)$  via two principal mechanisms: 1) muon energy loss in the Pb by ionization decreasing  $P(\mu \rightarrow e)$  and dominating at low momentum; 2) bremsstrahlung in Pb increasing  $P(\mu \rightarrow e)$  and dominating at high momentum.

To estimate the  $K_{\mu2}$  background contamination, the kinematic suppression factor is computed with the standard setup simulation, while the validated simulation of muon interaction in the LKr is employed to account for  $P(\mu \rightarrow e)$  suppression. Uncertainty of the background estimate is due to the limited size of the data sample used to validate the simulation.

**$K_{\mu2}$  decay followed by  $\mu \rightarrow e$  decay** contributes significantly to the background. However energetic forward daughter positrons compatible to  $K_{e2}$  topology are suppressed due to muon polarization<sup>12</sup>.

**$K_{e2\gamma}$  (SD) decay**, a background by  $R_K$  definition, has a rate similar to that of  $K_{e2}$ : the world average<sup>7</sup> is  $\text{BR} = (1.52 \pm 0.23) \times 10^{-5}$ . Theoretical rate calculations depend on the form factor model, and have a similar precision. Energetic positrons ( $E_e^* > 230$  MeV in  $K^+$  frame) with  $\gamma$  escaping detector acceptance contribute to the background. MC background estimation has a 15% uncertainty due to limited knowledge of the process. A recent measurement by KLOE<sup>8</sup>, published after announcement of the NA62 preliminary result, is not used.

**Beam halo** background in the  $K_{e2}$  sample induced by halo muons (undergoing  $\mu \rightarrow e$

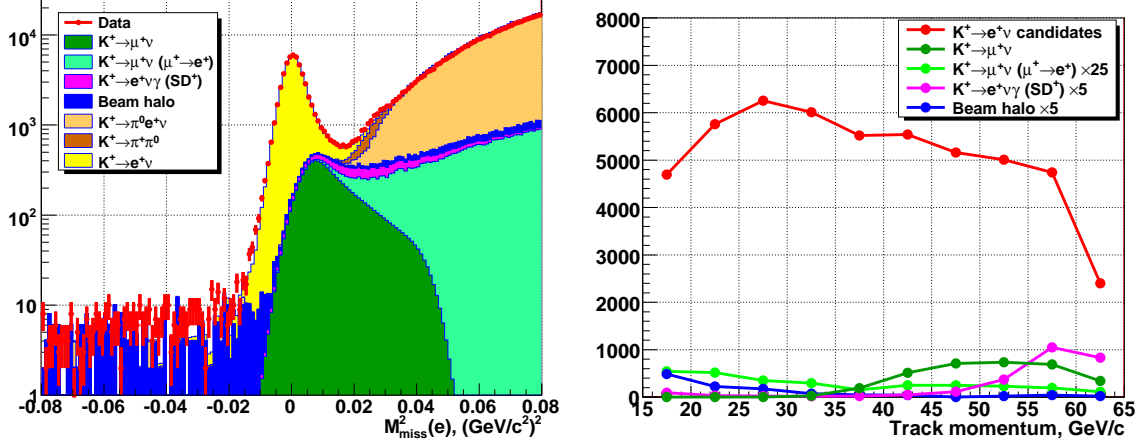


Figure 2: (a) Reconstructed squared missing mass distribution  $M_{\text{miss}}^2(e)$  for the  $K_{e2}$  candidates: data (dots) presented as sum of MC signal and background contributions (filled areas). (b) Numbers of  $K_{e2}$  candidates and background events in lepton momentum bins.

Source	$N_B/N_{\text{tot}}$	Source	$N_B/N_{\text{tot}}$	Source	$N_B/N_{\text{tot}}$
$K_{\mu 2}$	$(6.28 \pm 0.17)\%$	$K_{e2\gamma}$ (SD)	$(1.02 \pm 0.15)\%$	$K_{e3}$	0.03%
$K_{\mu 2} (\mu \rightarrow e)$	$(0.23 \pm 0.01)\%$	Beam halo	$(1.45 \pm 0.04)\%$	$K_{2\pi}$	0.03%
Total background: $(8.03 \pm 0.23)\%$					

Table 1: Summary of the background sources in the  $K_{e2}$  sample.

decay in flight or mis-identified) is measured directly by reconstructing  $K_{e2}^+$  candidates from a control  $K^-$  data sample collected with the  $K^+$  beam dumped. Background rate and kinematical distribution are qualitatively reproduced by a halo simulation. The uncertainty is due to the limited size of the  $K^-$  sample. Beam halo is the only significant background source in the  $K_{\mu 2}$  sample, measured to be 0.25% (with a negligible uncertainty) with the same technique as for  $K_{e2}$  decays.

The number of  $K_{e2}$  candidates is  $N(K_{e2}) = 51,089$  (about four times the statistics collected by KLOE <sup>8</sup>) and  $N(K_{\mu 2}) = 15.56 \times 10^6$ . The  $M_{\text{miss}}^2(e)$  distributions of data events and backgrounds are presented in Fig. 2a. Backgrounds integrated over lepton momentum are summarized in Table 1; their distributions over lepton momentum are presented in Fig. 2b.

#### 4 Systematic uncertainties

**Positron identification efficiency** is measured directly as a function of momentum and LKr impact point using pure samples of electrons and positrons obtained by kinematic selection of  $K^+ \rightarrow \pi^0 e^+ \nu$  decays collected concurrently with the  $K_{e2}$  sample, and  $K_L^0 \rightarrow \pi^\pm e^\mp \nu$  decays from a special  $K_L^0$  run of 15 hours duration. The  $K^+$  and  $K_L^0$  measurements are in good agreement. The measured  $f_e$  averaged over the  $K_{e2}$  sample is  $(99.20 \pm 0.05)\%$ . Muon identification inefficiency is negligible.

**The geometric acceptance correction**  $A(K_{\mu 2})/A(K_{e2})$  is strongly affected by the radiative  $K_{e2\gamma}$  (IB) decays. A conservative systematic uncertainty is attributed to approximations used in the  $K_{e2\gamma}$  IB simulation. The resummation of leading logarithms <sup>10</sup> is not taken into account, however no systematic error is ascribed due to that. An additional systematic uncertainty reflects the precision of beam line and apparatus description in the MC simulation.

**Trigger efficiency** correction  $\epsilon(K_{e2})/\epsilon(K_{\mu 2}) = 99.9\%$  accounts for the fact that  $K_{e2}$  and  $K_{\mu 2}$  decay modes are collected with different trigger conditions: the  $E > 10$  GeV LKr energy

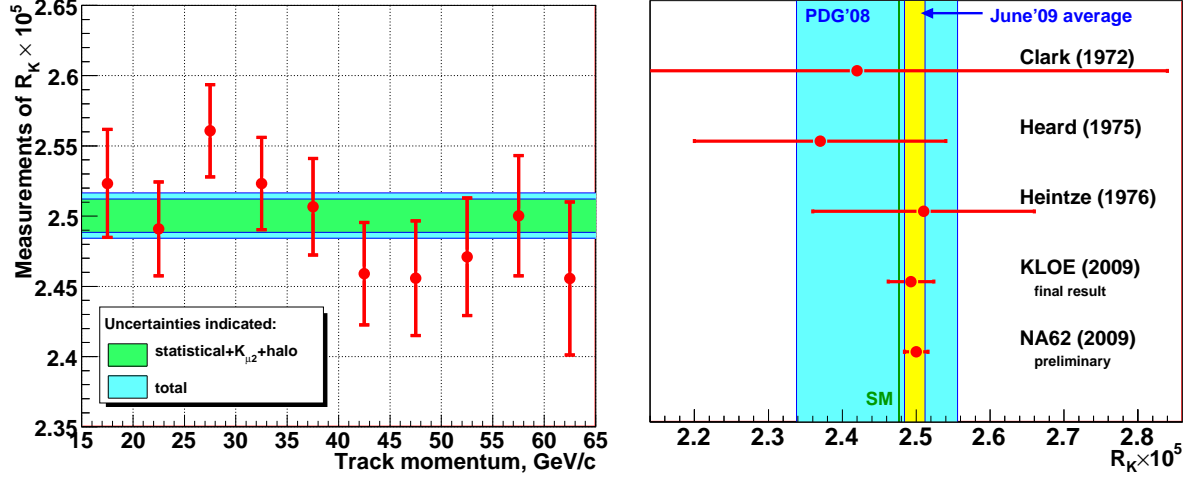


Figure 3: (a) Measurements of  $R_K$  in lepton momentum bins. (b) The world average of  $R_K$ .

Source	$\delta R_K \times 10^5$	Source	$\delta R_K \times 10^5$	Source	$\delta R_K \times 10^5$
Statistical	0.012	Beam halo	0.001	Geom. acceptance	0.002
$K_{\mu 2}$	0.004	Positron ID	0.001	Trigger dead time	0.007
$K_{e2\gamma}$ (SD)	0.004	IB simulation	0.007		

Table 2: Summary of uncertainties of  $R_K$ : statistical and systematic contributions.

deposition signal enters the  $K_{e2}$  trigger only. A conservative systematic uncertainty of 0.3% is ascribed due to effects of trigger dead time which affect the two modes differently. **LKr global readout efficiency**  $f_{\text{LKr}}$  is measured directly to be  $(99.80 \pm 0.01)\%$  and stable in time using an independent LKr readout system.

## 5 Result and conclusions

The independent measurements of  $R_K$  in lepton momentum bins, and the result combined over the momentum bins are presented in Fig. 3a. The uncertainties of the combined  $R_K$  are summarised in Table 2. The preliminary result is  $R_K = (2.500 \pm 0.012_{\text{stat.}} \pm 0.011_{\text{syst.}}) \times 10^{-5} = (2.500 \pm 0.016) \times 10^{-5}$ , which is consistent with the SM expectation. Analysis of the whole 2007–08 data sample is expected to decrease the uncertainty of  $R_K$  down to 0.4%. A summary of  $R_K$  measurements is presented in Fig. 3b: the current world average is  $(2.498 \pm 0.014) \times 10^{-5}$ .

## References

1. W.S. Hou, Phys. Rev. **D48** (1993) 2342.
2. G. Isidori and P. Paradisi, Phys. Lett. **B639** (2006) 499.
3. V. Cirigliano and I. Rosell, Phys. Rev. Lett. **99** (2007) 231801.
4. A. Masiero, P. Paradisi and R. Petronzio, Phys. Rev. **D74** (2006) 011701.
5. A. Masiero, P. Paradisi and R. Petronzio, JHEP **0811** (2008) 42.
6. J. Ellis, S. Lola and M. Raidal, Nucl. Phys. **B812** (2009) 128.
7. C. Amsler *et al.* (PDG), Phys. Lett. **B667** (2008) 1.
8. F. Ambrosino *et al.*, Eur. Phys. J. **C64** (2009) 627. Erratum-ibid. **C65** (2010) 703.
9. V. Fanti *et al.*, Nucl. Instrum. Methods **A574** (2007) 433.
10. C. Gatti, Eur. Phys. J. **C45** (2006) 417.
11. S.R. Kelner, R.P. Kokoulin and A.A. Petrukhin, Phys. Atom. Nucl. **60** (1997) 576.

12. L. Michel, Proc. Phys. Soc. **A63** (1950) 514.